NANO LETTERS

2007
Vol. 7, No. 7
2152−2156

# NanoSQUIDs Based on Niobium Constrictions

**Aico G. P. Troeman,* Hendrie Derking, Bert Borger, Johannes Pleikies, Dick Veldhuis, and Hans Hilgenkamp**

*Faculty of Science and Technology and Mesa+ Institute for Nanotechnology, University of Twente, P.O. Box 217, 7500 AE Enschede, The Netherlands*

*Received April 13, 2007; Revised Manuscript Received June 5, 2007*

**ABSTRACT**

**Superconducting quantum interference devices (SQUIDs) based on niobium nanobridges have been produced by means of focused ion beam milling. Typical critical currents of 4–25 $\mu$A and flux sensitivities of 40–200 $\mu V/\Phi_0$ were measured for sensors based on 80 nm wide, 50 nm thick, and 150 nm long bridges. A white flux noise level of 1.5 $\mu\Phi_0/Hz^{1/2}$ was measured for a device with an area of 900 $\mu m^2$ and a critical current of 15 $\mu$A. The effective area of the smallest produced SQUID was $3.6 \times 10^{-2}$ $\mu m^2$. Possible applications for such miniature SQUIDs are in scanning SQUID microscopy and the study of magnetic nanoparticles.**

Recent interest in the development of small-sized superconducting quantum interference devices (SQUIDs) has been motivated by the applicability of these sensors for investigations of small, local magnetic signals such as the magnetization reversal of small magnetic clusters[1−4] and the observation of local magnetic structures using a scanning SQUID microscope (SSM).[5−9] For both the aforementioned types of experiments, further miniaturization of the sensors offers a possibility to enhance the resolution of the experiment. Also, the realization of miniaturized SQUIDs patterned in three dimensions, e.g., on the tip of an AFM cantilever, could significantly improve the resolution of SSM systems.

The size of SQUIDs based on conventional superconductor−insulator−superconductor (SIS) tunnel junctions is limited by the lithography process. Even if the junctions can be miniaturized, achieving a sufficiently high critical current ($I_0$) poses a limitation on the size of an eventual SQUID. On the basis of a standard 4.5 kA/cm$^2$ process,[10] a 100 × 100 nm$^2$ junction would have an $I_0$ of approximately 0.5 $\mu$A. For $T = 4.2$K and $I_0 = 0.5$ $\mu$A, the noise parameter $\Gamma = 2\pi k_b T/I_0\Phi_0$, describing the ratio between the thermal and Josephson coupling energies in a junction, would have a value of approximately 0.35. From the literature, however, it is known that quantum effects in SQUIDs are only observable for $\Gamma \lesssim 0.2$.[11]

Superconducting nanobridges, exhibiting nontrivial current−phase relationships and high current densities,[12] can be very suitable alternatives to tunnel junctions. These structures can be created in a single nanopatterning step. By patterning two of such constrictions in a miniature superconducting ring a DC SQUID with submicrometer effective area ($A_{eff} = \Phi_0/H_0$, where $\Phi_0 = h/2e(\approx 2 \times 10^{-15}$ Tm$^2$) and $H_0$ is the magnetic field required to complete one period in the SQUID voltage−field ($V-H$) characteristic), can be created.

SQUIDs based on nanobridges, patterned with electron beam lithography (EBL), have been reported in literature.[1−3,5−7,13−16] The smallest $A_{eff}$ of these sensors is 0.5−1 $\mu$m$^2$. Recently, also, small SQUIDs with carbon nanotubes as junctions have been reported,[4] but these sensors were not really miniaturized in terms of $A_{eff}$. In this letter, SQUIDs based on niobium nanobridges, produced by focused ion beam (FIB) milling, are described. Even though, in comparison to state of the art systems, the resolution of the used FIB system is modest, the small sizes of the realized devices prove the potential of the technique. Because FIB nanopatterning is not limited to flat surfaces (as demonstrated, e.g., in ref 17), similar SQUIDs with three-dimensional geometries could, potentially, be created.

All structures described in this article are patterned in 50 nm thick, 5 $\mu$m wide Nb leads, prepared on oxidized Si substrates by DC sputtering and standard photolithography with lift-off. The FIB system used to pattern the devices is based on a Ga ion source (FEI type 83-2LI EVA). All experiments were conducted at a beam voltage of 25 kV and a beam current of 41 pA. The corresponding ion beam diameter was 150 nm with a full width at half-maximum of the ion distribution profile of 50 nm. All the described electronic characterizations were performed at $T = 4.2$ K with the sample immersed in liquid helium.

From previous studies, it is known that the superconducting properties of Nb are suppressed by the implantation of Kr[18] and N[19] into interstitial lattice sites. The described

* Corresponding author. E-mail: A.G.P.Troeman@TNW.Utwente.nl.

10.1021/nl070870f CCC: $37.00 
**Published on Web 06/15/2007**

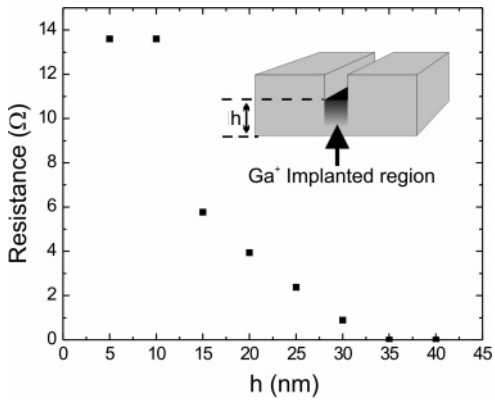


**Figure 1.** Resistance at $T = 4.2$ K of 1 $\mu$m wide trenches in 50 nm thick niobium striplines (inset) as a function of the thickness $h$ of the remaining Nb.

suppression of the critical temperature ($T_c$) is attributed to disorder effects resulting from slight induced changes in the lattice parameter ($a$) of the Nb structures (typically $\Delta a/a \approx$ 1%). To evaluate the extent to which Ga implantation affects the properties of patterned devices, calculations were performed using SRIM.[20] Simulation of the impact of $10^4$ Ga ions, with 25 keV energies, at normal incidence to a 50 nm Nb layer, revealed that the average implantation depth is 10−15 nm inward from the surface of the film; 2.5% of the ions reach depths of 25 nm and 0.4% is implanted as far as 30 nm inward from the surface of the structure.

To experimentally determine the effect of the Ga implantation on a patterned Nb device, trenches of 1 $\mu$m widths and different depths were milled in 5 $\mu$m wide prestructured Nb striplines of 50 nm thickness. This allows for a systematic variation of the remaining Nb height ($h$). Estimated values for $h$ are based on the calibrated linear etch rate for the specific patterning process (Nb, 25 keV $Ga^+$ FIB). From the dependence of the resistance versus $h$ (Figure 1), it can be concluded that, at $T = 4.2$ K, superconductivity is suppressed as far as 30 nm or more inward from the surface. This corresponds to the calculated implantation depth mentioned above. Combined with the prediction that only 0.4% of the ions reach this far into the structure, the known FIB beam current and corresponding Nb etching rate (41 pA and 6.7 $\times$ $10^{-3}$ $\mu m^3$/s), this means that an implantation of roughly 1.1 $\times$ $10^7$ Ga ions into the bottom 5 nm of a patterned 1 $\times$ 5 $\mu m^2$ wide trench (which equals 1.6 $\times$ $10^9$ Nb atoms) is enough to suppress the superconducting properties of the structure at $T = 4.2$ K. This corresponds to an implantation ratio of approximately 0.7%, which is of the same order of magnitude as the reported values for Kr (0.2−2%) and N (0.5−5%).

Superconducting nanobridges behave much like Josephson elements. The nature of the current−phase relationship (CPR) in these structures is determined by their dimensions.[12] The CPR in bridges with small lengths ($l$) and widths ($w$) is expected to be single-valued and sinusoidal. In longer, narrow bridges ($l \gtrsim 3\ \xi$, $w \lesssim 4\ \xi$, where $\xi$ is the superconducting coherence length) the CPR is multivalued and the result of localized phase-slippage of the order parameter in the center of the bridge. In long structures with widths of several

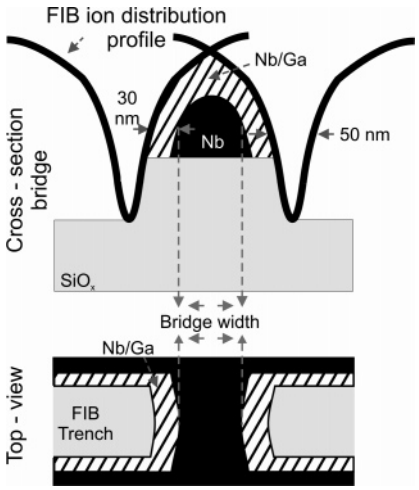


**Figure 2.** Schematic of the nanobridge patterning principle and definition of designed bridge width.

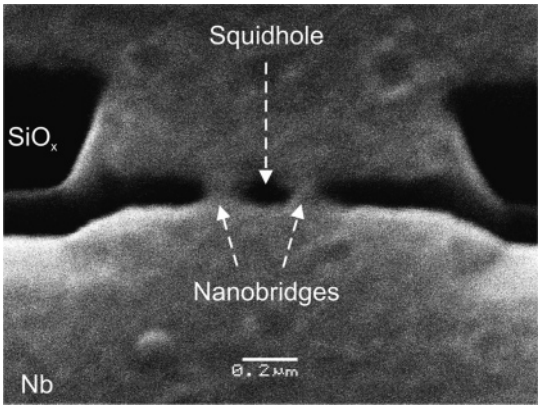


**Figure 3.** Scanning electron micrograph of a SQUID based on niobium nanobridges with designed widths of 80 nm. The effective area of this device is 3.6 $\times$ $10^{-2}$ $\mu m^2$.

coherence lengths ($l \gtrsim 3\ \xi$, $w \gtrsim 4\ \xi$), the coherent motion of vortices across the bridge is expected to determine the CPR. Measurements of the CPR in our Nb nanobridges are described elsewhere.[21] The exact nature of these relationships is, however, of lesser importance for the realization of the SQUIDs, as their operation is merely based on the incorporation of elements with a nontrivial CPR in a superconducting ring.

The Nb nanobridges are patterned by letting two ion beam profiles overlap.[22] This allows for the creation of structures with smaller dimensions than the diameter of the FIB. Because the sidewalls of the nanobridges are also patterned from above, a suppression of the superconducting properties of the nanobridges as far as 30 nm inward from the surface is taken into account, see Figure 2. The length of the bridges corresponds to the ion beam diameter of 150 nm.

In Figure 3, a scanning electron micrograph of the smallest obtained SQUID is shown. It is based on two nanobridges with 80 nm designed widths, separated by a hole with a diameter corresponding to the beam size (150 nm). In Figure 4A, its $I-V$ characteristics for different applied fields and the voltage−applied field ($V$-H) modulations are shown. Because of the small size of the SQUID, the maximum

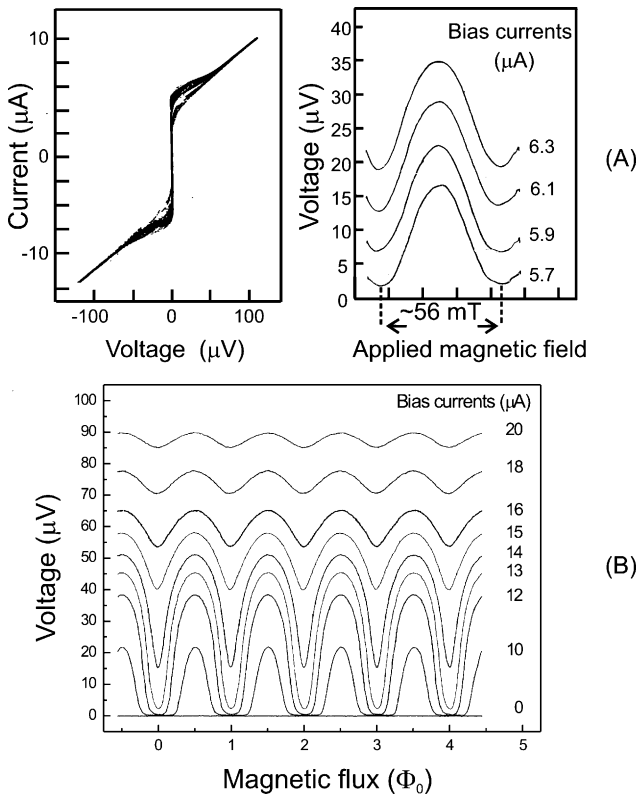


**Figure 4.** (A) $I-V$ curve for different values of the applied magnetic field and the corresponding $V-H$ characteristics of the device shown in Figure 3. (B) $V-H$ characteristics of a reference SQUID, also based on 80 nm wide bridges but with an effective area of 5 $\mu$m$^2$.

applicable magnetic field in our setup (approximately 75 mT) corresponds to an applied flux of about 1.5 $\Phi_0$ through the SQUID loop.

The effective area of this SQUID, determined from the periodicity of the $V-H$ characteristics, is approximately 3.6 $\times$ $10^{-2}$ $\mu$m$^2$. This is more than twice as large as the hole size (1.6 $\times$ $10^{-2}$ $\mu$m$^2$). However, if an increase of the hole diameter due to the implantation of Ga ions into the edge (2 $\times$ 30 nm) is taken into account, the calculated area is 3.5 $\times$ $10^{-2}$ $\mu$m$^2$, which is comparable to the determined effective area. The characteristics shown in part B correspond to a reference device with an effective area of 5 $\mu$m$^2$ based on nanobridges with the same designed widths.

Typically, the approximation of the maximum SQUID sensitivity is based on the value of the screening parameter $\beta_L = 2I_cL/\Phi_0$. On the basis of literature,[14] it can be expected that the total inductance of miniature nanobridge based SQUIDs is dominated by the contributions of the kinetic inductances of the bridges, which is given by $L_k \approx 1/\pi\,(\Phi_0 l/(\pi I_c \xi(T)))$[12] (with $l$ the bridge length and $\xi(T)$ the coherence length). On the basis of this formula, for the device discussed above ($l \approx 150$ nm and $\xi(T) \approx 37$ nm), a total kinetic inductance of 150 pH can be estimated, yielding a calculated value of $\beta_L \approx 0.75$. For such values of $\beta_L$, $dV/d\Phi_{max}$ can be estimated by $2\beta_L/(1+\beta_L)\,R/L$,[23] which results in $dV/d\Phi_{max} \approx 115\ \mu V/\Phi_0$. This value is of the same order of magnitude as the measured value.

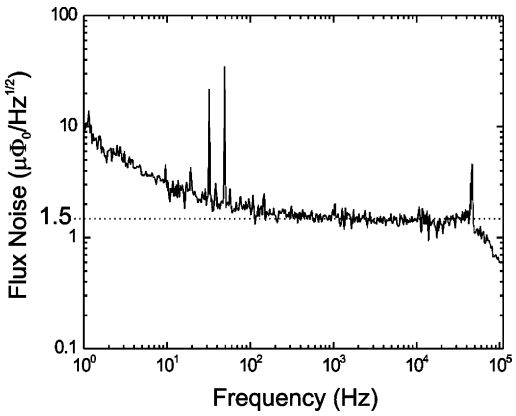


**Figure 5.** Flux noise spectral density measured at $T = 4.2$ K for a nanobridge-based SQUID with a critical current of 15 $\mu$A and an area of 900 $\mu$m$^2$.

Considerable variations in the properties of both aforementioned devices can be noted ($I_{c,A} \approx 5\ \mu$A, $I_{c,B} \approx 10\ \mu$A; $dV/d\Phi_{max,A} \approx 50\ \mu V/\Phi_0$, $dV/d\Phi_{max,B} \approx 160\ \mu V/\Phi_0$). Critical currents ranging from 4 to 30 $\mu$A, maximum magnetic sensitivities ranging from 40 to 200 $\mu V/\Phi_0$, and modulation depths of up to 50 $\mu$V have been measured for SQUIDs based on 80 nm wide bridges. These numbers are based on the characterization of approximately 20 devices (with $A_{eff} \approx$ 900 $\mu$m$^2$, $\approx 1\ \mu$m$^2$, and $\approx 3.6 \times 10^{-2}\ \mu$m$^2$). The described spread in the properties of devices based on bridges with the same designed widths is caused by the limitations posed by the FIB patterning process. Because the eventual nanobridges are smaller than the beam diameter, any irregularities in the beam properties during patterning can lead to significant differences in the sizes and shapes of the eventual bridges.

The electronic characteristics of six SQUIDs ($A_{eff} \approx 900$ $\mu$m$^2$ (3$\times$) and $\approx 1\ \mu$m$^2$ (3$\times$)) were monitored over the course of time. No significant degradation of the measured sensor properties was noted, which seems to exclude degradation due to a gradual oxidation of the Nb or inward diffusion of implanted Ga ions. However, after several months and cooldowns, most SQUIDs became defective from one cooldown to the other. The reasons for this are unclear, but we expect them to be of accidental rather than intrinsic nature. For devices with $I_c \geq 25\ \mu$A, hysteretic $I-V$ characteristics were measured, which do not allow for conventional current−biased $V-\Phi$ measurements. The hysteresis is believed to be caused by thermal heating associated with phase-slippage of the superconducting order parameter in the structure.[24]

Noise measurements were performed on a nanobridge-based SQUID with a critical current of 10 $\mu$A, a sensitivity of approximately 160 $\mu V/\Phi_0$, and an area of 900 $\mu$m$^2$, using a conventional DC SQUID with an integrated flux transformer[25] as a low-temperature pre-amplifier. The nanobridge-based SQUID was inductively coupled to this flux transformer (mutual inductance $M \approx 8.7$ nH). In Figure 5, the measured flux noise spectrum exhibiting a white noise level of 1.5 $\mu\Phi_0/Hz^{1/2}$ is displayed. This value is significantly larger than the determined noise limit of the setup ($\approx$ 0.2

$\mu\Phi_0/\mathrm{Hz}^{1/2}$). A $1/f$ corner frequency of about 80 Hz can be determined from the spectrum. Because $1/f$ critical current noise due to the trapping of electrons is expected to be negligible in a barrier-free configuration, the dominant contribution to the total level of $1/f$ noise is expected to be associated with the trapping and subsequent hopping of electrons in defect states in the superconducting material.[26] A high $1/f$ corner frequency could then be related to damage induced to the device during the patterning process.

The inductance of the SQUID washer is estimated to be 63 pH,[27] yielding a calculated energy resolution of $7.6 \times 10^{-32}$ Js ($\approx$ 115 h). The measured white level of the flux noise spectral density is approximately a factor of 3 higher than what would be expected for RSJ tunnel junction based SQUIDs, in which the noise contribution is dominated by the Johnson noise in the resistors ($S_\Phi^{1/2}(\omega) \approx (16k_BTR)^{1/2}/(dV/d\Phi)$).[22] For this estimate, a value of $R/2 \approx 10\ \Omega$, which is the normal state resistance ($R_N$) of the described device, was used. Such a comparison is only relevant if $R_N$ is predominantly determined by the nonsuperconducting Ga-implanted Nb shunting the actual nanobridge. On the basis of the measured values for the resistance of the different patterned trenches displayed in Figure 1, this could well be the case. The resistance of a trench with $h \approx 30$ nm is approximately 1 $\Omega$. Given its length ($l \approx 150$ nm) and width ($w \approx 5\ \mu$m), this yields a resistivity $\rho = R\,\sigma/l \approx 10^3\ \Omega$ nm. Here $\sigma$ is the cross-sectional area. For a Nb bridge with $l \approx 150$ nm, $w \approx 80$ nm, covered by 30 nm nonsuperconducting Ga-implanted material, the estimated resistance then is $R = \rho\ l/\sigma \approx 16\ \Omega$. This yields a device normal state resistance of $R/2 \approx 8\ \Omega$, which is comparable to the measured value for $R/2$. However, the origin of $R_N$ in the described SQUIDs has not been verified directly, which makes the presented discussion nonconclusive.

As described before, a possible application for miniaturized SQUIDs is for the detection of small clusters of magnetic particles. For such experiments, the spin sensitivity of the sensor, which is given by $S_n^{1/2}(\omega) = 2aS_\Phi/\mu_B\mu_0$,[28] with "$a$" the width of the SQUID loop, is an important figure of merit. For miniature EBL-based nanobridge SQUIDs low values for $S_\Phi^{1/2}(\omega)$, and thus also for $S_n^{1/2}(\omega)$, have been reported in literature ($S_\Phi^{1/2}(\omega) \approx 0.4\ \mu\Phi_0/\mathrm{Hz}^{1/2}$, $S_n^{1/2}(\omega) \approx 70\ \mu_B/\mathrm{Hz}^{1/2}$,[29] and $S_\Phi^{1/2}(\omega) \approx 5\ \mu\Phi_0/\mathrm{Hz}^{1/2}$, $S_n^{1/2}(\omega) \approx 200\ \mu_B/\mathrm{Hz}^{1/2}$).[30] The described values for $S_\Phi^{1/2}(\omega)$ are of the same order of magnitude as the measured white noise level of our device. Combined with the fact that all realized devices are based on the same type of Josephson element, the flux noise spectral density reported above for the 900 $\mu$m$^2$ SQUID can be used to estimate the possible spin sensitivity of smaller sensors. A device with an area of $3.6 \times 10^{-2}\ \mu$m$^2$ would have a spin sensitivity of about 50 $\mu_B/\mathrm{Hz}^{1/2}$, which would be even lower than the values reported above. If, in addition, $S_\Phi^{1/2}(\omega)$ scales with the device inductance in a similar fashion as is the case for tunnel junction based SQUIDs ($S_\Phi^{1/2}(\omega) \sim L^2$, for $\beta_L \approx 1$),[22] even smaller values for $S_n^{1/2}(\omega)$ could be achieved. It should be noted that the discussed definition of $S_n^{1/2}(\omega)$ is based on calculations for geometries where a single magnetic dipole is located in the center of the SQUID loop. Optimal flux coupling, and thus higher values for $S_n^{1/2}(\omega)$, can be obtained for a configuration where the dipole is located directly on top of the nanobridge.[4] In practice, thus, the spin sensitivity of the experiment is determined by the location of the magnetic particles with respect to the SQUID geometry.

In conclusion, SQUIDs based on Nb nanobridges, patterned by means of FIB milling, have been created. The Ga ion implantation depth, associated with the FIB patterning process, was predicted and measured to be as large as 30 nm. Furthermore, it was measured that a relative Ga implantation of 0.7% in a Nb device is enough to suppress its superconducting properties at $T = 4.2$ K. SQUIDs with effective areas as small as $3.6 \times 10^{-2}\ \mu$m$^2$ have been created, exhibiting typical critical currents of up to 30 $\mu$A and maximum magnetic sensitivities of 40−200 $\mu\mathrm{V}/\Phi_0$. A white noise level of 1.5 $\mu\Phi_0/\mathrm{Hz}^{1/2}$ was measured for a SQUID with a critical current of 15 $\mu$A and an area of 900 $\mu$m$^2$.

**Acknowledgment.** We acknowledge helpful discussions with D. Tilbrook and S. Lam. This work was supported by The Netherlands Organization for Scientific Research (NWO) through a VIDI grant.

## References

(1) Jamet, M.; Wernsdorfer, S.; Thirion, C.; Mailly, D.; Dupuis, V.; Mélinon, P.; Pérez, A. *Phys. Rev. Lett.* **2000**, *86*, 4676−4769.
(2) Gallop, J.; Josephs-Franks, P. W.; Davies, J.; Hao, L.; MacFarlane, J. *Phys. C* **2002**, *368*, 109−113.
(3) Lam, S. K. H.; Tilbrook, D. L. *Appl. Phys. Lett* **2003**, *82*, 1078−1080.
(4) Cleuziou, J.-P.; Wernsdorfer, W.; Bouchiat, V.; Ondarharçu, T.; Nonthioux, M. *Nat. Nanotechnol*. **2006**, *1*, 53−59.
(5) Dechert, J.; Krischker, K.; Göddenhenrich, T.; Mück, M.; Heiden, C. *IEEE Trans. Appl. Supercond.* **1997**, *7*, 3143−3146.
(6) Hasselbach, K.; Veauvy, C.; Mailly, D. *Phys. C* **2000**, *332*, 140−147.
(7) Veauvy, C.; Hasselbach, K.; Mailly, D. *Rev. Sci. Instrum*. **2002**, *73*, 3825−3830.
(8) Chen, K.; Magnelind, P.; Larsson, P.; Tzalenchuk Ya, A.; Ivanov, Z. G. *Phys. C* **2002**, *372−376*, 63−67.
(9) Hilgenkamp, H.; Ariando Smilde, H.-J.; Blank, D.; Rijnders, G.; Rogalla, H.; Kirtley, J.; Tsuei, C. C. *Nature* **2003**, *422*, 50−53.
(10) *Hypres Niobium Integrated Circuit Fabrication; Process no. 03-10-45 Design Rules, Revision 23*; *Hypres: Elmsford, N*, 2006.
(11) Clarke, J.; Koch, R. H. *Science* **1988**, *242*, 217−223.
(12) Likharev, K. K. *Rev. Mod. Phys* **1979**, *51*, 101−159.
(13) Voss, R. F.; Laibowitz, B.; Ketchen, M. B.; Broers, A. N. *Superconducting Quantum Interference Devices and Their Application*; Hahlbohm, H. D., Luebbig, H., Eds.; de Gruyter: New York, 1980; pp 365−380.
(14) Claassen, J. H. *Appl. Phys. Lett* **1982**, *40*, 839−841.
(15) Dilorio, M. S.; de Lozanne, A.; Beasley, M. R. *IEEE Trans. Magn.* **1983**, *MAG-19*, 308−311.
(16) Rogalla, H.; David, B.; Rühl, J. *J. Appl. Phys.***1984**, *55*, 3441−3443.
(17) Blamire, M. G. *Supercond. Sci. Technol*. **2006**, *19*, S132−S137.
(18) Heim, G.; Kay, E. *J. Appl. Phys* **1975**, *46*, 4006−4012.
(19) Camerlingo, C.; Scardi, P.; Tosello, C.; Vaglio, R. *Phys. Rev. B.* **1985**, *31*, 3121−3123.
(20) Ziegler, J. F.; Biersack, J. P.; Littmark, U. *The Stopping and Range of Ions in Solids*; Pergamon Press: New York, 1985.
(21) Troeman, A. G. P.; van der Ploeg, S.; Il'Ichev, E.; Golubov, A. A.; Hilgenkamp, H. Temperature Dependent Measurements of the Supercurrent−Phase Relationship in Niobium Nanobridges; in press.
(22) Blank, D. H. A.; Booij, W.; Hilgenkamp, H.; Vulink, B.; Veldhuis, D.; Rogalla, H. *IEEE Trans. Appl. Supercond*. **1995**, *5*, 2786−2789.

(23) Tesche, C. D.; Clarke, J. *J. Low Temp. Phys*. **1977**, *29*, 301−331.
(24) Hasselbach, K.; Mailly, D.; Kirtley, J. R. *J. Appl. Phys*. **2002**, *91*, 4432−4437.
(25) Pleikies, J.; Usenko, O.; Kuit, K. H.; Flokstra, J.; de Waard, A.; Frossati, G. SQUID Developments for the Gravitational Wave Antenna MiniGRAIL. *IEEE Trans. Appl. Supercond*. **2007**, accepted for publication.
(26) Koch, R. H.; DiVicenzo, D. P.; Clarke, J. Model for 1/*f* Flux Noise in SQUIDs and Qubits **2005**, cond-mat/0702025.
(27) Ketchen, M. B. *IEEE Trans. Magn.* **1987**, *23*, 1650−1657.
(28) Ketchen, M. B.; Awschalom, D. D.; Gallagher, W. J.; Kleinsasser, A. W.; Sandstorm, R. L.; Rozen, J. R.; Bumble, B. *IEEE Trans. Magn.* **1989**, *25*, 1212−1215.
(29) Voss, R. F.; Laibowitz, R. B.; Boers, A. N.; Raider, S. I.; Knoedler, C. M.; Viggiano, J. M. *IEEE Trans. Magn.* **1981**, *MAG-17*, 395−399.
(30) Lam, S. K. H. *Supercond. Sci. Technol*. **2006**, *19*, 963−967.

NL070870F